Bulletin of the Seismological Society of America. Vol. 66, No. 4, pp. 1133 1144. August 1976

TECTONIC IMPLICATIONS OF THE BRAWLEY EARTHQUAKE SWARM, IMPERIAL VALLEY, CALIFORNIA, JANUARY 1975

By Carl E. Johnson and David M. Hadley

ABSTRACT

The Brawley earthquake swarm provided a unique opportunity for studying a highly interesting tectonic region. The swarm was most intense for a period of 4 days including 75 events with M_L between 3.0 and 4.7 with a spatial extent of 12 km. Precise relative hypocenters were obtained for 264 earthquakes ($M_L \geq 1.5$) using a master event method to calibrate the USGS Imperial Valley array. These locations together with well-constrained focal mechanisms for 16 of the largest events suggest faulting on at least three distinct structures. Hypocentral depths ranged from 4 to 8 km, compared to a basement depth of about 6 km for this part of the Imperial Valley. The swarm began on a nearly vertical right-lateral fault striking N8°W (Brawley fault) about 8 km southeast of Brawley at a point which had experienced enhanced shallow seismicity during the preceding 4 days. The seismicity migrated bilaterally north and south from this point at a constant velocity of 0.5 km/hr terminating to the north on a steeply south dipping, N50°E-striking fault. This structure is on trend with splays associated with the northern end of ground breakage of the 1940 Imperial Valley earthquake. To the south the seismicity ended near the northern end of the 10 km of surface rupture mapped by R. V. Sharp, which continues on strike to a point near the Imperial fault. Tectonic interpretations include the transfer of right-lateral offset from the Imperial fault to the Brawley fault associated with the formation of a closed depression bounded on the west and east by these two faults.

Introduction

The Brawley swarm, a sequence of earthquakes with no distinct main shock, occurred in the Imperial Valley near the community of Brawley between January 23 and 31, 1975. Although there were scattered events both before and after, this period is associated with the highest level of seismic activity. The largest event ($M_L = 4.7$) occurred about 5 hr after the onset of the swarm and was both preceded and followed by events with magnitudes greater than 4. The level of seismicity during the swarm fluctuated considerably, with bursts of tightly clustered intense activity. Globally, swarms are often associated with magmatic activity such as that associated with oceanic ridges (Sykes, 1970; Thatcher and Brune, 1971) and active geothermal areas (Ward and Bjornsson, 1971).

Seismicity within the Imperial Valley is characterized by both swarm activity and main-shock aftershock sequences (Hileman *et al.*, 1973; Richter, 1958). There is evidence that both patterns of activity can occur on the same structure, as appears to be the case for the Imperial fault. The Brawley swarm was not unusually large compared to earlier swarms within the Imperial Valley. It is, however, the largest swarm that has occurred since April of 1973 when the dense 16-station USGS Imperial Valley seismic array was installed. Other swarms that have occurred since the installation of this array are discussed by Hill *et al.*, (1975a, 1975b).

The Imperial Valley is part of the Gulf of California physiographic province. It is not a simple grabben-like structure bounded by normal faults (Sharp, 1972) as one might infer

from geomorphological considerations. Rather, crustal extension is accommodated by strike-slip motion on vertical faults striking obliquely to the axis of the valley. South of the Imperial Valley similar faults appear to offset active ridge segments (Henley and Bischoff, 1973; Bischoff and Henley, 1974). The high heat flow within the Imperial Valley (Rex, 1970) suggests similar processes may be occurring there. Whatever these tectonic processes may be, they are obscured by the great accumulation of sediments in this part of the Imperial Valley (Biehler *et al.*, 1964). Because of this a detailed analysis of the seismicity such as is presented here is of special significance.

Analysis of Data

The conclusions expressed in this paper are based on accurate relative hypocenters for the events of the swarm and first-motion focal mechanisms for those events large enough to be observed regionally. The primary data were the arrival times and polarities of *P*

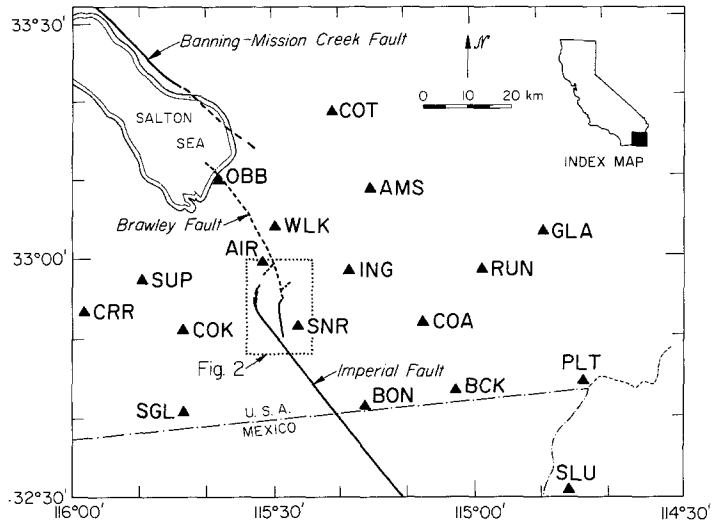

FIG. 1. Map showing station distribution (solid triangles), observed surface faulting including that of the 1940 Imperial Valley earthquake (solid lines), and faults inferred from seismic evidence (dashed lines). The dotted rectangle outlines the area shown in greater detail in Figure 2.

waves recorded by the 16 short-period vertical seismometers comprising the USGS Imperial Valley array (Hill *et al.*, 1975b). The signals from this array are telemetered to Caltech and recorded by develocorders on 16-mm film. The average station spacing is about 25 km and is roughly centered on the vicinity of the swarm (Figure 1) with excellent coverage in all azimuths. There were generally 10 stations within 50 km of most events providing excellent hypocentral control. These data are supplemented by *T* (trigger) and *S* times taken from strong-motion accelerograms written at AIR (Figure 1) on January 25. These data are discussed by Johnson and Hanks (1976) who believe that the trigger times are delayed by no more than 0.1 to 0.2 sec from the actual *P* times. The data from this instrument were particularly important in establishing "master events" for the relative location method discussed later. The first-motion data set was enhanced by readings from various short-period vertical seismometers operated by Caltech and the USGS throughout southern California. Additional first-motion data from within the Imperial Valley were provided by J. Combs and C. Helsley (personal communication) from an array of nine 10-day recorders located near the Mesa Geothermal Anomaly.

In order to achieve a high level of accuracy in the calculation of hypocenters, arrival times at the stations of the Imperial Valley array were read with considerable care. All events were read by one individual to eliminate variations due to differences in criteria for picking the onset of P waves. Events were read at the same screen position on one viewer to avoid problems associated with slight distortions in magnification. Only impulsive arrivals were included in the study. In this manner a repeatability with a standard deviation of about 0.01 sec could be realized.

The relative location method used in this study was simple, yet effective and easy to apply. The procedure consists of three parts. First one or more events are selected and designated "master events". The selection criterion is primarily the availability of impulsive P and S arrival times at as many stations as possible. For routine aftershock studies, for example, a well-recorded aftershock occurring subsequent to augmented local instrumentation could be selected for this purpose. This event is then located as accurately as possible. Next the working assumption is made that the calculated travel-time residuals are due solely to fixed station delays. The remaining events are then located using these delays and the suite of stations used in locating the master event. This procedure is precisely equivalent to fitting a relative location vector to arrival-time differences between an event and a master event. The major goal of this approach is to calculate accurate relative hypocenters so as to provide a clearer picture of the fault relationships associated with a sequence of events.

The advantages of this technique are manifold. The fit of the relative location vector is nonlinear yet can easily be implemented with any hypocentral location program capable of using station delays. Near-station effects are removed from the problem by differencing the travel times. Inadequacies in the crustal velocity model are similarily reduced to second order so that distant stations can be included with the same weighting as nearer ones without biasing the location.

The relative location method was implemented using the earthquake location program "HYPO71", an iterative stepwise regression designed by Lee and Lahr (1975), and a crustal velocity model appropriate for the Imperial Valley. We were fortunate in having a refraction study (Westmoreland profile of Biehler *et al.*, 1964) within 10 km of the swarm. This profile provided a crustal velocity model from the surface to a 6.4-km/sec basement at a depth of 5.9 km. The velocity structure shown in Table 1 is essentially this model, although large-velocity discontinuities have been smoothed by introducing thin gradational layers in order to minimize destabilizing effects on the focal mechanism determinations.

Two events ($M_L = 4.3$ at 1431 GMT on January 25 and $M_L = 4.0$ at 1230 GMT on January 23) were selected as master events. The hypocenters for these two events are given in Table 2. The epicenters of most of the other events of the swarm were within 3 km of one or the other of the two master events.

The first master event (1431 GMT) was located using the *a priori* delays shown in Table 2 along with the strong focal depth control provided by the $S - T$ time at the 3-component station AIR at an epicentral distance of 1.3 km. The *a priori* delays were determined from a consideration of the location of a station with respect to the deep, sediment-filled basin represented by the Imperial Valley together with what was known about the near station crustal structure. Without these delays, anomalously deep hypocenters would have been calculated due to early arrivals at the periphery of the valley. The total delays shown in Table 2 were calculated by summing the relative delays (travel-time residuals from the location of the master event) and the *a priori* delays. These total delays were used to locate the second master event (1230 GMT) relative to the first. The total delays for the second master event (Table 2) were similarly calculated, and the remaining events were then

located relative to the closer master event. For relative locations involving as many as 12 stations the root mean square of the arrival time residuals was typically about 0.02 sec with an associated estimate of location error of from 100 to 300 meters. This error is comparable to that expected from reading errors alone and attests to the internal consistency of arrival-time differences as an unbiased data set.

TABLE 1

CRUSTAL VELOCITY MODEL USED FOR EVENT LOCATIONS AND FOCAL MECHANISM DETERMINATIONS

Velocity (km sec)	Depth to Top of Layer (km)
2.2	0.0
3.8	1.7
4.7	3.1
4.9	4.0
5.2	5.0
5.5	5.3
5.8	5.8
6.3	6.1
6.4	7.0
6.5	8.0
6.6	9.0
6.7	10.0
7.8	25.0

TABLE 2

MASTER EVENT LOCATIONS AND STATION DELAYS (IN SECONDS) USED FOR RELATIVE LOCATIONS

		Master Event 1		Master Event 2	
Date		Jan. 25, 1975		Jan. 23, 1975	
Origin (GMT)		1431h, 1.01s		1230h, 16.02s	
Latitude		32° 59.15′		32° 56.00′	
Longitude		115° 30.02′		115° 28.88′	
Depth		5.96 km		4.00 km	
Magnitude		4.3		4.0	
Station	A Priori Delay	Relative Delay	Total Delay	Relative Delay	Total Delay
AIR	0.00	−0.11	−0.11	—	—
AMS	−0.30	0.03	−0.27	−0.02	−0.32
CRR	−0.30	0.01	−0.29	0.08	−0.22
COA	0.30	−0.05	0.25	−0.01	0.29
COK	0.30	−0.09	0.21	—	0.30
ING	0.15	0.04	0.19	0.03	0.18
OBB	0.10	−0.10	0.00	−0.12	0.02
PLT	−0.30	−0.08	−0.38	−0.02	−0.32
RUN	0.00	−0.08	−0.08	−0.10	−0.10
SGL	−0.20	−0.04	−0.24	−0.15	−0.35
SLU	0.30	0.00	0.30	0.03	0.33
SNR	0.00	0.21	0.21	0.21	0.21
SUP	−0.50	0.09	−0.41	0.13	−0.37
WLK	0.00	0.14	0.14	0.15	0.15

The effect of mislocation of the master events was assessed by adding a "mislocation vector" to the master event hypocenter and then recalculating the relative locations using revised total delays. In all cases the pattern of relative locations was essentially unchanged with each event translated by an amount comparable to the original "mislocation

vector". From this we infer that a mislocation of the master event by as much as 1 to 2 km would shift the pattern of hypocenters spatially but would not alter the results of this study.

First-motion focal mechanisms for the larger events of the swarm were calculated with a program developed by Jan Garmany and Jim Whitcomb (discussed by Whitcomb, 1973) using takeoff angles and azimuths provided by "HYPO71". This program exhaustively searches the model space of possible fault plane orientations. Graphic output of the optimal solution, as well as plots showing goodness of fit for various possible orientations of slip vectors, tension, and compression axes, permit evaluation of the degree of constraint for each solution.

It was found that considerable care was required in the calculation of crustal focal mechanisms. The main source of difficulty was associated with miscalculation of focal depth. Variation in takeoff angle as a hypocenter is moved through a sharp discontinuity in the crustal velocity model can cause a point (station) originally near the center of the focal sphere to plot on the periphery. This can be disastrous for all but pure strike-slip mechanisms. Smoothing of sharp discontinuities in structure by inserting thin gradational layers was found to have a considerable stabilizing effect on the focal mechanism calculations. Coupled with the enhanced depth control provided by the relative location method, the problem was almost entirely obviated. The most constrained focal mechanisms are shown together with their supporting data in Figure 3. Their relationship to the seismicity, shown in Figure 5, is the basis for the discussion in the next section.

Magnitudes were used in this study to assess the relative importance of the events comprising the swarm and to select events for focal mechanism determination. Since precise magnitudes were not required, a reasonable estimate was obtained by establishing an empirical linear relationship between the log of signal duration measured at station LTC (Little Chuckwalla) and local magnitudes from the torsion seismometer at Glamis for 20 events ranging in magnitude from 2.5 to 4.7. The station LTC is part of the USGS western Mojave array and lies at a distance of 70 ± 2 km from the events of the swarm. According to the relationship between duration and magnitude discussed by Lee *et al.*, (1972) this variation in epicentral distance would be expected to introduce an error in magnitude of less than 0.1. A larger source of error arose as a result of the short intervals between some events. This caused magnitudes to be underestimated when the signal coda was truncated by a subsequent large event and overestimated when later smaller events appeared to extend the signal coda.

Spatial Distribution of Events

The epicenters of the located earthquakes are plotted in Figure 2 together with topographic contours, the concurrent surface breakage mapped by Sharp (1975), and the surface faulting associated with the 1940 Imperial Valley earthquake. Three distinct lineations, indicated by broken lines, are apparent in the epicentral distribution. With the additional evidence provided by focal mechanisms, three fault structures have been inferred from these lineations although no surface expression has been observed. The absence of surficial features is not surprising considering recent sedimentation and agricultural modification in this part of the Imperial Valley.

The prominent northwest trending lineation is identified as the Brawley fault discussed by Hill *et al.*, (1975a, 1975b). Its strike of about N8 W is compatible with those of the focal mechanisms for events 1 through 6 of Figure 3. These events are associated spatially with the Brawley fault (Figure 4), and the mechanisms require right-lateral motion on a nearly

vertical fault plane. To the south this trend is continued by the surface cracks reported by Sharp (1975) to a point about 1.4 km north of its apparent intersection with the Imperial fault northeast of El Centro. The character of these cracks according to Sharp implies a tectonic origin with right-lateral offset. The absence of epicenters along that portion of the Brawley fault where cracks were observed implies their development was associated with an aseismic process such as creep, although slip at depth at its southern end may have occurred during a swarm occurring in August of 1975. As pointed out by Sharp (1976), the occurrence of surficial cracks was coincident with that portion of the Brawley fault

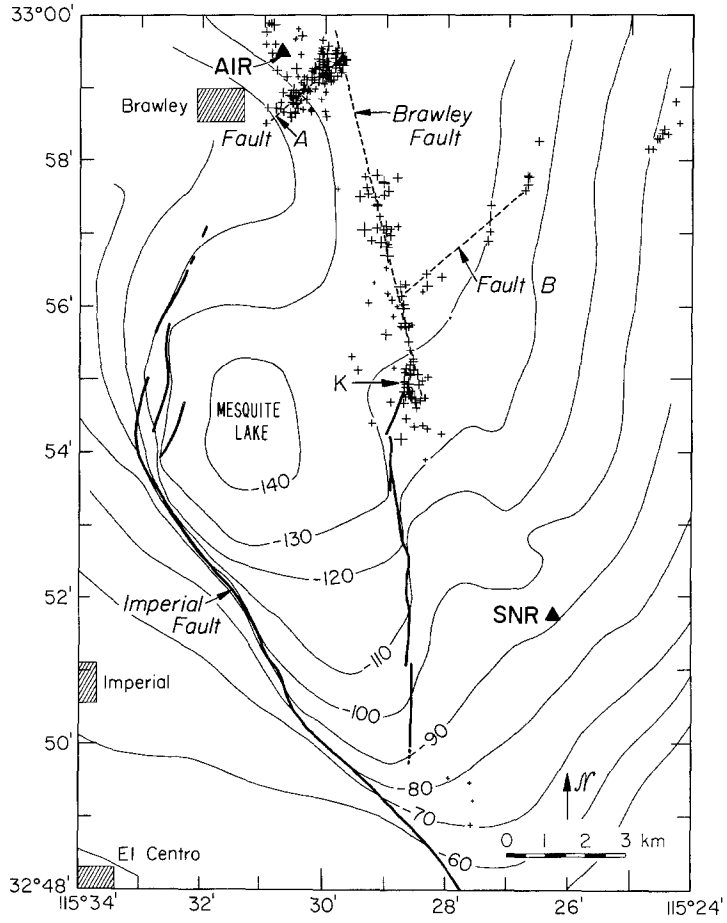

FIG. 2. Detailed map showing epicenters associated with the Brawley swarm (plus signs, size proportional to magnitude), observed surface faulting (heavy lines), faults inferred from seismicity (dashed lines), and topographic contours (light lines). The letter "K" indicates the point where the surface faulting coincident with the Brawley swarm crossed Keystone Road.

manifesting a well-developed pre-existing scarp. This is also apparent in Figure 2 from the correlation between topography and surface faulting. The 1.4-km gap between the southern end of the observed cracks and the Imperial fault was filled by a sequence of four events ($M \leqq 3.2$) on January 31 (Figure 2), 7 days after the beginning of the swarm.

North of Brawley the trend of the Brawley fault is continued by the alignment of events reported by Hill *et al.*, (1975a, 1975b), shown as a dashed line on Figure 1. This alignment continues to a point just south of the Salton Sea with a strike that becomes progressively more westerly until it approaches that of the Imperial fault. From its northernmost point

south to its intersection with the Imperial fault the Brawley fault appears to be active for a distance of about 40 km.

The two northeast-striking lineations have been designated fault A and fault B (Figure 2) for reference purposes in the following discussion. Events 7, 8, 9, 12, 13, 14, 15, and 16 of Figure 3 are representative of focal mechanisms calculated for events associated with fault A. If the selection of the fault plane is based on the trend of the epicenters, then the thrust mechanisms occurring on a north dipping plane early in the sequence are replaced by a combination of normal and left-lateral motion on a south dipping plane at the end of the

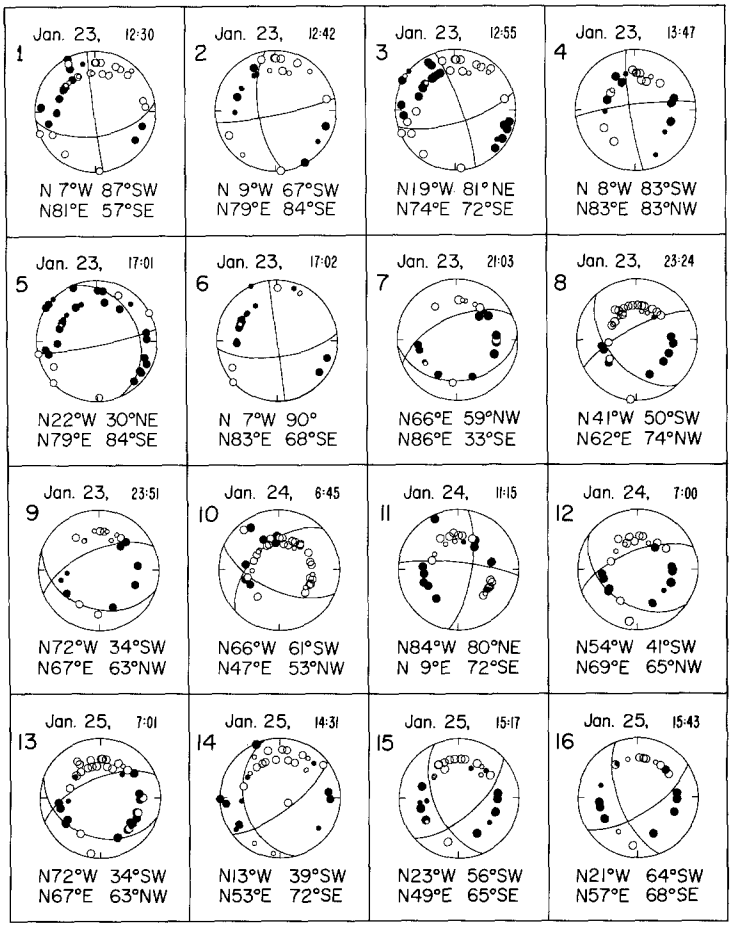

FIG. 3. Lower hemisphere equal-area projection of first-motion data and focal mechanisms. Solid circles indicate compression, open circles indicate dilatation. The fault plane orientations are not listed in order of preference.

swarm. There is some indication that the north dipping plane is truncated by the south dipping one, but the scatter in the hypocenters is too great to provide convincing evidence for this assertion. The strike of fault A is on trend with northeast trending splay faults that formed at the northern end of the ground breakage associated with the 1940 Imperial Valley earthquake (Ulrich, 1941; Buwalda and Richter, unpublished manuscript).

MIGRATION AND TEMPORAL CHANGES

Figure 4 displays the temporal and spatial variation in the seismicity distribution and focal mechanisms that developed in the course of the Brawley swarm, perhaps the most

interesting phenomena observed. The lower portion of Figure 4 is a plot of the distance along the Brawley fault as a function of origin time for the events occurring during the 4 days of peak activity. Distance along the Brawley fault is defined as the epicentral distance from a point (32°48′N, 115°27′W) near the Imperial fault on trend with the Brawley fault. This plot has been divided into nine time frames spanning the first 3 days. The events occurring within each time interval are plotted in the corresponding plan view on the *upper* portion of Figure 4 showing the relationships to the inferred fault structures shown on Figure 2. The tick marks along the Brawley fault indicate the distance along the fault in kilometers and correspond to those marking the ordinate of the lower portion of the figure.

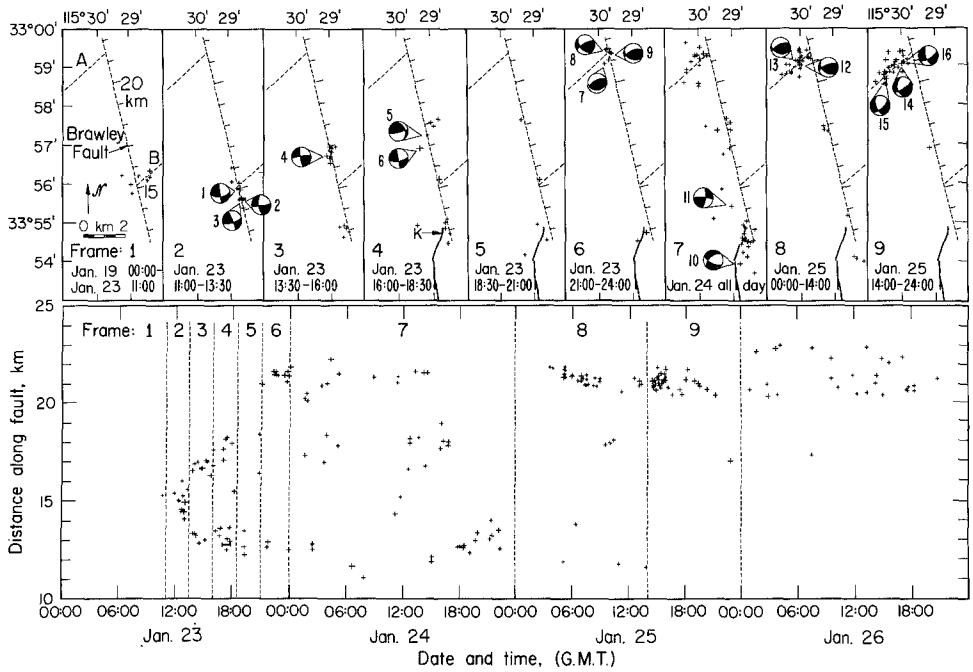

FIG. 4. Spacio-temporal relationships associated with the events of the Brawley swarm. In the *lower* portion of the figure the distance along the Brawley fault is plotted as a function of origin time (size proportional to magnitude). The first 3 days are divided into nine time frames separated by dashed lines. The epicenters of the events in each time frame are plotted in the *upper* portion of the figure. The tick marks along the inferred faults (dashed line) correspond to those marking the ordinate of the lower plot. The reference numbers associated with the focal mechanism correspond to those in Figure 3. Solid quadrants are compressional.

One of the most intriguing results of this study is the well-defined migration of the onset of seismicity bilaterally north and south along the Brawley fault from its point of inception near the intersection of the Brawley fault and fault B (frames 2 through 6). To the north the migration covered a distance of 6.5 km in about 13 hr, giving a propagation velocity of 0.5 km/hr. The swarm was preceded by a gradual increase in shallow seismicity ($h < 6$ km) in the immediate vicinity of the intersection of the Brawley fault and fault B (frame 1) during the 4 days prior to the onset of peak activity. Spatially these events appear to lie on a plane dipping steeply to the north with strike coincident with fault B. The character of the seismicity changed abruptly at 1230 GMT on January 23 with a sudden increase in the number and magnitude of events (frame 2). These and subsequent events were deeper ($h > 6$ km) with a distinct tendency to align along the strike of the Brawley fault. This trend is supported by the strike of the focal mechanisms. In order to better represent the onset of

seismicity as it progressively involved more of the Brawley fault, the remainder of January 23 is divided into $2\frac{1}{2}$-hr intervals (frames 2 through 6). The passage of the onset of seismicity was characterized by a sudden increase in activity followed by a return to relative quiet. Shallower events tended to trend off the strike of the Brawley fault in a manner suggestive of conjugate failure within the sediments. The migration to the south terminated near the northern end of the surface cracks. Sharp (1975) was able to bracket the time of the formation of the scarp at Keystone Road (marked with a "K" on Figure 2 and frame 4 of Figure 4) to the interval 1700–1800 GMT on January 23. This interval is shown as a bracket on the lower portion of Figure 4. The development of the scarp occurred about 3 hr after the projected arrival of the disturbance at a depth of about 5 km. The delay may be related to the propagation time from this depth to the surface. The time of formation of the cracks farther south is not known.

To the north, the absence of events in frame 5 is associated with the passage of the disturbance along a portion of the Brawley fault near kilometer 20 that was quiet throughout the swarm as shown in Figure 4. The northward migration terminated at the intersection of the Brawley fault and fault A with a tightly clustered sequence of events shown in frame 6. Focal mechanisms and the alignment of these events indicate reverse faulting on a northeast striking plane dipping steeply to the north.

Frame 7 shows the diffuse pattern of events occurring on January 24. Of note is the onset of shallow seismicity ($h < 6$ km) along the strike of fault A. This was followed on January 25 by two rather distinct bursts of activity (frames 8 and 9) with depths ranging from 6 to 8 km. By midday on January 25 the focal mechanisms for events associated with fault A are predominantly "normal" with a component of left-lateral slip (frame 9).

Tectonic Implications

Several studies (Lomnitz *et al.*, 1970; Elders *et al.*, 1972) have postulated the existence of a chain of offset ridge segments and transform faults connecting similar structures in the Gulf of California with the Banning-Mission Creek branch of the San Andreas fault. Hill *et al.*, (1975a) concluded that the Brawley fault was an important link in this chain. Triangulation data at the northern end of the Brawley fault are consistent with fault slip occurring at a constant rate of 4.5 mm/yr with a cumulative offset of 20 cm since 1934 (Savage *et al.*, 1974). Evidence from the Brawley swarm supports these results while at the same time providing considerable insight into the relationship between the Brawley fault and the Imperial fault (Figure 1). Right-lateral motion on these two structures is consistent with the tectonic formation of the closed depression known as Mesquite Lake (Figure 2). The vertical motion associated with the 1940 Imperial Valley earthquake (Ulrich, 1941), the sense of vertical motion reported by Sharp (1975), and the focal mechanisms reported in the present study are all compatible with the active subsidence of a triangular block bounded on the southwest by the Imperial fault, on the east by the Brawley fault, and on the northwest by fault A.

The mechanical relationship among these faults provides a possible explanation for the northeasterly trending splays that developed at the northern end of the surface breakage associated with the 1940 Imperial Valley earthquake (Figure 2). The observation that these splays are on strike with fault A, and the close spatial relationship of these two features suggest a common structure. This implies that slip along the northern end of the Imperial fault may have terminated with conjugate motion on fault A.

Both the focal mechanisms and the distribution of hypocenters suggest that the seismically active portion of the Brawley fault is a vertical plane striking N8 W. Figure 5

shows the distribution of the events of the Brawley swarm projected onto this plane. The definition of distance along the fault is the same as that used in Figure 4. The events are distributed over a well-defined depth zone ranging from 4 to 8 km, compared to a basement depth of 6 km. A depth of 8 km may be the limiting depth for failure by brittle fracture in this portion of the Imperial Valley. The transition from brittle fracture to plastic flow is governed largely by temperature. A limiting depth of 8 km is consistent with the generally higher heat flow in the Imperial Valley as compared to other areas of southern California where earthquakes occur to depths of 15 km.

Fault structures detailed in this study may have important consequences for understanding geothermal resources in the Imperial Valley. The possibility of fault structures acting as conduits for geothermal brines has been suggested by Combs and Hadley (1975) for the Mesa Geothermal Anomaly. Hill *et al.*, (1975a) have commented on the proximity of the Brawley fault and the Brawley geothermal area. The region of highest heat flow associated with the Brawley geothermal area northeast of Brawley (Rex, 1970) includes the intersection of the Brawley fault and Fault A. Figure 4 (frame 6) shows that

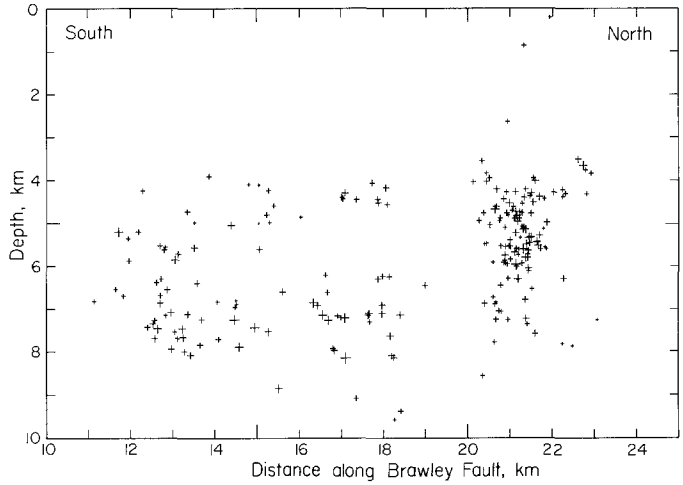

FIG. 5. Hypocenters associated with the Brawley swarm projected onto the fault plane of the Brawley fault. Character size is proportional to magnitude.

this intersection was a point of concentrated seismic activity. Such a structure should be considered as a candidate for the vertical transport of the hot brines feeding the Brawley geothermal area. The events associated with this intersection were shallower than 6 km, consistent with the locally greater heat flow.

The temporal variations in seismicity observed during the Brawley swarm deserve further consideration. When projected on the plane of the Brawley fault the events preceding the swarm are generally confined to an area less than 1 km in diameter. With the onset of increased activity the seismically active region of the Brawley fault gradually expanded from the area of initial seismicity (Figure 4). This expansion was characterized by the seismic activation of small regions or patches along the plane of the Brawley fault. These patches remained active for periods ranging up to about 1 hr before returning to a low level of seismicity. Other portions of the fault plane were aseismic throughout the Brawley swarm.

One model capable of explaining these observations is the propagation of a right-lateral creep event in the plane of the Brawley fault. Passage of the leading edge of the creep event is marked by the associated seismic activation of regions capable of failing by brittle

fracture. The observation that seismically quiet regions of the fault plane were traversed without apparently effecting the rupture velocity suggests these portions of the fault slipped aseismically as opposed to being "locked". The thesis that aseismic slip occurred on the plane of the Brawley fault is supported by the lack of seismicity associated with the 10 km of surface cracking mapped by Sharp (1975).

Acknowledgments

We would like to thank C. R. Allen, T. Hanks, D. Hill, and R. Sharp for many useful discussions and preprints of papers. Data provided by the U.S. Geological Survey from the Imperial Valley array was critical in pursuing this study.

This research was supported under U.S. Geological Survey Contract 14-08-0001-14142.

References

Biehler, S., R. L. Kovach, and C. R. Allen (1964). Geophysical framework of the northern end of the Gulf of California structural province, in *Marine Geology of Gulf of California*, T. Van Andel and G. Shor, Editors, *Am. Assoc. Petrol. Geologists Mem. 3* 126–296.

Bischoff, J. L. and T. L. Henyey (1974). Tectonic elements of the central part of the Gulf of California, *Bull. Geol. Soc. Am.* **85**, 1893–1904.

Combs, J. and D. M. Hadley (1975). Microearthquake investigation of the Mesa Geothermal Anomaly, Imperial Valley, California, *Geophysics* (in press).

Elders, W. A., R. W. Rex, Tsvi Meidav, P. T. Robinson, and S. Biehler (1972). Crustal Spreading in Southern California, *Science* **178**, 15–24.

Henyey, T. L. and J. L. Bischoff (1973), Tectonic elements of the northern part of the Gulf of California, *Bull. Geol. Soc. Am.* **84**, 315–330.

Hileman, J. A., C. R. Allen, and J. M. Nordquist (1973), *Seismicity of the Southern California Region, 1 January 1932 to 31 December 1972*, Seismological Laboratory, California Institute of Technology, 487 p.

Hill, D. P., P. Mowinckel, and L. G. Peake (1975a). Earthquakes, active faults, and geothermal areas in the Imperial Valley, California, *Science* **188**, 1306–1308.

Hill, D. P., P. Mowinckel, and K. M. Lahr (1975b), Catalog of Earthquakes in the Imperial Valley, California, *U.S. Geological Survey Open-File Report*, Washington, D.C., 29 p.

Johnson, D. and T. Hanks (1976). Strong-motion accelerograms of the Brawley swarm: January 25, 1975, *Bull. Seism. Soc. Am.* **65**, 1155–1158.

Lee, W. H. K., R. E. Bennet, and K. L. Meagher (1972). A Method of Estimating Magnitude of Local Earthquakes from Signal Duration, *U.S. Geological Survey Open-File Report*, Washington, D.C., 28 p.

Lee, W. H. K., and J. C. Lahr (1975). HYPO71 (Revised): A Computer Program for Determining Hypocenter, Magnitude, and First Motion Pattern of Local Earthquakes, *U.S. Geological Survey Open-File Report*, Washington, D.C., 113 p.

Lomnitz, C., F. Mooser, C. Allen, and W. Thatcher (1970). Seismicity and tectonics of the northern Gulf of California region, Mexico. Preliminary results, *Geofis. Int.* **10**, 37–48.

Rex, R. W. (1970), *Investigation of Geothermal Resources in the Imperial Valley and Their Potential Value for Desalination of Water and Electricity Production*, University of California, Riverside, 14 pp.

Richter, C. F. (1958), *Elementary Seismology*, Freeman, San Francisco, 768 pp.

Savage, J. C., D. Goodreau, and W. H. Prescott (1974), Possible fault slip on the Brawley Fault, Imperial Valley, California, *Bull. Seism. Soc. Am.* **64**, 713–715.

Sharp, R. V. (1972), Tectonic Setting of the Salton Trough, in the Borrego Mountain Earthquake of April 9, 1968. *U.S. Geol. Surv. Profess. Paper 787*, 3–15.

Sharp, R. V. (1976). Surface faulting in Imperial Valley during the earthquake swarm of January-February, 1975. *Bull. Seism. Soc. Am.* **66**, 1145–1154.

Sykes, L. R. (1970). Earthquake swarms and sea floor spreading, *J. Geophys. Res.* **75**, 6598–6609.

Thatcher, W. and J. N. Brune (1971). Seismic study of an oceanic ridge earthquake swarm in the Gulf of California, *Geophys. J.* **22**, 473–489.

Ulrich, F. P. (1941). The Imperial Valley earthquakes of 1940, *Bull. Seism. Soc. Am.* **31**, 13–31.

Ward, P. L. and S. Bjornsson (1971). Microearthquakes, swarms, and geothermal areas of Iceland, *J. Geophys. Res.* **76**, 3953–3982.

Whitcomb, J. (1973). Part I. A Study of the Velocity Structure of the Earth by the Use of Core Phases. Part II. The 1971 San Fernando Earthquake Series Focal Mechanisms and Tectonics, *PhD Thesis*, California Institute of Technology, 368 p.

SEISMOLOGICAL LABORATORY
CALIFORNIA INSTITUTE OF TECHNOLOGY
PASADENA, CALIFORNIA 91125
DIVISION OF GEOLOGICAL AND PLANETARY SCIENCES CONTRIBUTION NO. 2701.

Manuscript received December 1, 1975